Journal of
Composites Science

MDPI

Article

Effects of Grapevine Fiber and Additives on the Properties of Polylactic Acid Green Bio-Composites

Chun-Wei Chang, Chien-Chung Huang, Yi-Jing Jiang, Po-Hsiang Wang and Yeng-Fong Shih *

Department of Applied Chemistry, Chaoyang University of Technology, No. 168, Jifeng E. Rd., Wufeng District, Taichung 41349, Taiwan; adad94033@gmail.com (C.-W.C.); othink168chien@gmail.com (C.-C.H.); n85132009@gmail.com (Y.-J.J.); roy900611@gmail.com (P.-H.W.)
* Correspondence: syf@cyut.edu.tw

Abstract: In recent years, numerous researchers have incorporated plant fibers into polymers to alter the thermal and mechanical properties of materials. Grapevines, considered agricultural waste, have led to burdens for farmers and environmental challenges due to their mass production. This study aims to reduce the brittleness of polylactic acid (PLA) by adding polybutylene succinate (PBS) as a toughening agent and employing grapevine fiber (GVF) as a biomass filler. Additionally, the influence of GVF, toughening agents, compatibilizers, and lubrication agents on the tensile strength, heat deflection temperature (HDT), and impact strength of the composites was examined. The findings revealed that the addition of 10% GVF and 5% PBS increased the impact and tensile strengths of PLA from 17.47 J/m and 49.74 MPa to 29.7 J/m and 54.46 MPa, respectively. Moreover, the HDT of the composites exceeded 120 °C when the GVF content was more than 40 wt%. Additionally, the inclusion of a compatibilizer and a lubrication agent enabled the composite containing 30% GVF to achieve tensile and impact strengths of 45.30 MPa and 25.52 J/m, respectively. Consequently, these GVF/PLA green bio-composites not only improve the mechanical and thermal properties of PLA but also promote the reuse of waste grapevines.

Keywords: poly(lactic acid); grapevine fiber; biomass filler; bio-composites

Citation: Chang, C.-W.; Huang, C.-C.; Jiang, Y.-J.; Wang, P.-H.; Shih, Y.-F. Effects of Grapevine Fiber and Additives on the Properties of Polylactic Acid Green Bio-Composites. *J. Compos. Sci.* **2024**, *8*, 422. https://doi.org/10.3390/jcs8100422

Academic Editors: Ahmed Koubaa, Mohamed Ragoubi and Frédéric Becquart

Received: 10 September 2024
Revised: 5 October 2024
Accepted: 11 October 2024
Published: 13 October 2024

1. Introduction

Food is an essential global resource, garnering significant attention from the United Nations. However, the substantial amount of agricultural waste generated from food cultivation remains a concern. The global volume of solid waste has significantly increased due to factors such as rapid population growth, accelerated urbanization, growing agricultural demand, and industrial expansion. The world's population is anticipated to reach 8.5 billion by 2030, by which solid waste generation is projected to hit 2.59 billion tons [1,2] Moreover, this figure is expected to double by 2050, reaching 4 billion tons [3]. Such an increase will further strain the already challenged environmental and climatic conditions. As a result, the development of methods for recycling solid waste is becoming increasingly urgent. In addition, the improper disposal of agricultural waste contributes to the production of greenhouse gases such as carbon dioxide, nitrous oxide, and methane, which pose threats to both human health and the natural environment [4]. In the past decade, over 40 countries have developed and adopted national policies, policy instruments, and strategies related to a new economic model. This model primarily focuses on efficient resource management, aiming to extend the useful life of materials and products, and prevent their value loss by integrating waste back into production processes [5].

Traditionally, farmers either directly burn this waste or convert it into carbonized nutrients for subsequent planting seasons. Unfortunately, these methods often result in considerable pollution and subsequent environmental harm [6]. Agricultural waste primarily consists of cellulose, lignocellulosic material, hemicellulose, pectin, and lignin, with cellulose being the most abundant polymer. The composition of agricultural waste

includes 30–40% cellulose, 30–50% hemicellulose, and 8–21% lignin. Given this composition, agricultural waste has significant potential for utilization in the production of various products. These include water-resistant gels, carbon fibers, bioplastics, bioactive natural products, coatings, foams, and both thermoplastic and thermosetting materials, all of which have wide-ranging industrial applications [7]. Therefore, integrating waste back into production processes is recognized as a means to promote sustainable agriculture.

Grapes are the world's second-largest fruit crop and are among the most widely cultivated fruits of economic value. For example, Spain alone produces over two million tons of waste annually from grape cultivation and wine production. This waste includes grape leaves and stems, lees, and winemaking wastewater [8,9]. While the lees and wastewater are repurposed for feed processing and water purification systems, grape leaves and stems are frequently discarded as waste [10]. Grapes are also a significant fruit crop in Taiwan, with cultivation taking place nearly year-round. The pruning period usually occurs from October to November. As a result, after a large harvest of grapes, there is also a considerable amount of grapevine waste generated from pruning. In Taiwan, grapes are economically important, with Changhua County being the primary cultivation area. A substantial amount of approximately 6000 tons per year of pruned vines is discarded as waste [11]. Although these pruned vines can be used as fertilizer, most of them are discarded, leading to environmental pollution. Therefore, we hope to reuse discarded grapevines and reintegrate them into grape agriculture, such as in products like grape trellises, water basins, seedling pots, and other items, in order to achieve the goals of a circular economy and sustainable agriculture. Prior research indicates that agricultural waste, such as plant fibers [12–14] or biochars [15], has been frequently incorporated into plastics to enhance material properties. Most traditional plastics are derived from petroleum chemicals, and the resulting plastic waste poses significant environmental harm. Consequently, biodegradable materials are gaining increased attention. Bioplastics, such as polylactic acid (PLA), are biodegradable, renewable, and sustainable alternatives to petroleum-derived plastics. PLA stands out among biodegradable polymers as it is sourced from renewable materials. Often referred to as corn starch resin, PLA can be derived from starch or carbohydrates such as wheat or sweet potatoes. Moreover, PLA offers properties and pricing comparable to conventional petrochemical plastics, making it the most widely utilized biodegradable polymer [16,17]. Nevertheless, PLA's high brittleness and poor thermal stability currently restrict its application range [18]. Polybutylene succinate (PBS) is widely recognized as a biodegradable material characterized by excellent ductility and heat resistance. PBS is synthesized through the condensation polymerization of succinic acid and butanediol. It easily undergoes decomposition and metabolization by various microorganisms in nature or enzymes, ultimately breaking down into carbon dioxide and water [19,20]. Furthermore, blending PBS with PLA has been shown to enhance the brittleness and thermal stability of PLA, thereby expanding its application range [21,22].

Adding plant fibers to biodegradable plastics to replace artificial fibers, such as glass and carbon fibers, and petroleum-derived resins, can create a fully bio-based composite material [23]. In addition to reducing material costs and increasing the utilization of natural resources, natural fibers also have carbon-neutralizing effects, which can lower product carbon emissions and enhance competitiveness [24]. However, the high polarity of plant fibers makes them incompatible with a low-polarity matrix like PLA or PBS [25]. Many researchers have improved the overall mechanical strength of materials by adding compatibilizers such as maleic anhydride-grafted PLA [16,25–27], maleic anhydride-grafted PBS [28,29], or surface modifications [30,31] to enhance interfacial adhesion. Additionally, adding lubricants to reduce melt viscosity improves the dispersion of plant fibers in the matrix, thereby enhancing the material's mechanical strength [32,33].

This study initially processes grapevines into grapevine fibers, then incorporates them into a PLA matrix. Moreover, the BiomassPla system certifies products that conform to standards set by the Japan BioPlastics Association (JBPA). One standard requires products to have a "biomass-based plastic ratio" of at least 25%. The JBPA defines "biomass-based

plastic ratio" as the proportion of the total weight consisting of components derived from biomass in the composition of the biomass-based plastic or biomass-derived thermosetting plastic raw material contained in the raw material and product (percentage by weight) [34]. Therefore, to effectively utilize agricultural waste and comply with BiomassPla certification, adding more biomass material (at least 25%) will be beneficial. The adhesion and dispersibility between the grapevine fibers and the PLA are enhanced through the addition of toughening agents, compatibilizers, and lubrication agents. This approach not only strengthens the mechanical and thermal properties of the material but also reduces material costs and increases the utilization rate of natural substances, contributing positively to overall environmental protection. The development of these materials aims to replace the widely used disposable plastic products with alternatives that enhance the lifecycle, added value, and economic benefits of biomass materials. This contributes to a sustainable agricultural management model and reduces the carbon footprint of products, further benefiting our natural environment.

2. Materials and Methods

2.1. Materials

The polylactic acid (PLA, PLA 2002D) with a density of 1.24 g/cm^3, melt flow index of 5–7 g/10 min at 210 °C, and a load of 2.16 kg was supplied by Nature-WorksLLC, and the polybutylene succinate (PBS, GP-9001N) was supplied by Minima Technology Co., Ltd., Taichung, Taiwan. Acetone, ethanol, methanol, isopropanol, dichloromethane, and xylene were purchased by Echo Chemical Co., Ltd., located in Miaoli, Taiwan. Maleic anhydride (MAH), benzoyl peroxide (BPO), and dicumyl peroxide (DCP) were provided from Alfa Aesar, MA, USA and were used without further purification. The lubrication agent (Licocare® RBW 330 powder TP VITA) was supplied by Clariant Specialty Chemical. The grapevines (Figure 1a) were obtained from Dacun Township, Changhua.

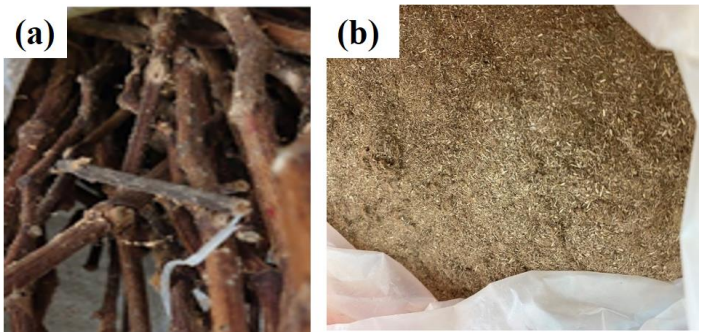

Figure 1. (**a**) Photographs of grapevines and (**b**) crushed and sieved grapevine powder.

2.2. Preparation of Grapevine Fiber (GVF)

First, the grapevines were dried in an oven, then crushed and ground. They were subsequently sieved using a 120-mesh sieve, followed by drying at 60 °C for 24 h to obtain grapevine fiber (GVF), as depicted in Figure 1b.

2.3. Preparation of Maleic Anhydride-Grafted Polybutylene Succinate (PBS-MA)

The procedure based on Shih et al. [15] 40 g of PBS and 4 g of MAH were pre-melted; subsequently, 0.5 g of benzoyl peroxide (BPO) was added in a counter-rotating internal mixer (Brabender PL2000, Duisburg, Germany) at 130 °C with a rotation speed of 50 rpm for 5 min. In order to remove the excess MAH, this obtained product was mixed with 200 mL of xylene in a three-neck bottle and refluxed at 85 °C for two hours. Afterward, the mixture was poured into acetone and rested for 40 min to obtain the refined maleic anhydride-grafted polybutylene succinate (PBS-MA). The reaction of maleic anhydride-grafted PBS was shown as Figure 2. The average grafting ratio (G_{MAH}, %) of MAH onto

PBS was determined to be 7.76% using the acid–base titration method [15]. The calculation method is shown in Equation (1):

$$G_{MAH} = 9.806\ (M_1V_1 - M_2V_2)/2m \quad (1)$$

where

M_1: Concentration of KOH–ethanol standard solution, mol/L
V_1: Titration volume of KOH–ethanol standard solution, mL
M_2: Concentration of HCl–isopropanol standard solution, mol/L
V_2: Titration volume of HCl–isopropanol standard solution, mL
m: Weight of PBS, g

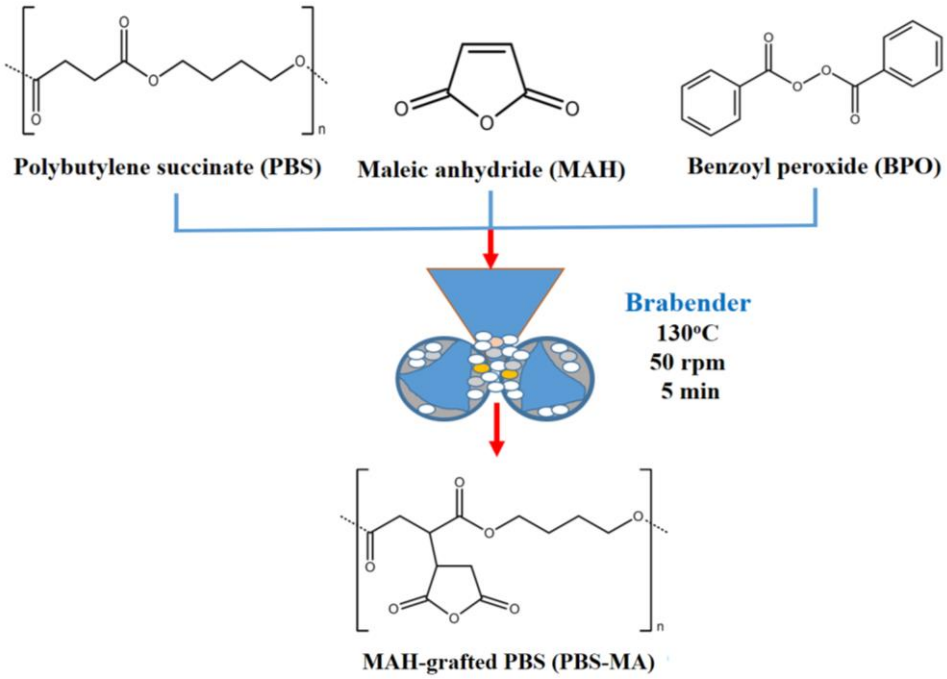

Figure 2. Preparation of MAH-grafted PBS.

2.4. Preparation of Maleic Anhydride-Grafted Polylactic Acid (PLA-MA)

An amount of 40 g of PLA and 4 g of MAH were pre-melted; subsequently, 0.56 g of dicumyl peroxide (DCP) was added in a counter-rotating internal mixer (Brabender PL2000, Duisburg, Germany) at 180 °C with a rotation speed of 50 rpm for 5 min. In order to remove the excess MAH, this obtained product was mixed with 200 mL of dichloromethane in a three-neck bottle, refluxed at 85 °C until completely dissolved, and precipitated in excess anhydrous ethanol to obtain the refined maleic anhydride-grafted polylactic acid (PLA-MA). The reaction of maleic anhydride-grafted PLA is shown in Figure 3. The average grafting ratio (G_{MAH}, %) of MAH onto PLA was determined to be 4.02% using the acid–base titration method, as shown in Equations (2) and (3) [35].

$$\text{Acid number (mg KOH/g)} = 56.1 \times M_{KOH} \times V_{KOH}/m \quad (2)$$

$$G_{MAH} = \text{Acid number} \times 98.06/(2 \times 561) \quad (3)$$

where

M_{KOH}: Concentration of KOH–methanol standard solution, mol/L
V_{KOH}: Titration volume of KOH–methanol standard solution, mL
m: Weight of PLA, g

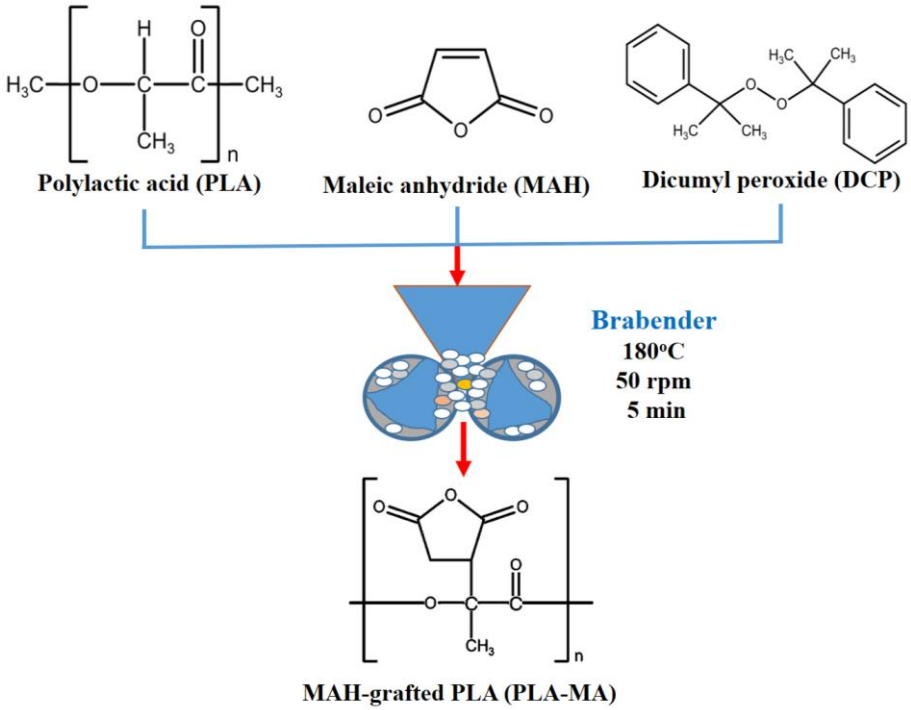

Figure 3. Preparation of MAH-grafted PLA.

2.5. Preparation of GVF/PLA Composites

The PLA, PBS, PBS-MA, PLA-MA, lubrication agent, and GVF were dried in an oven at 60 °C to achieve a moisture content of less than 1.0 wt%. They were then combined according to the formulation (wt%) outlined in Table 1 using a counter-rotating internal mixer (Brabender PL2000, Duisburg, Germany) at 175 °C and 50 rpm for 5 min, as depicted in Figure 4. The design of the formulation in Table 1 was based on the following factors: (1) using 3 or 5 wt% of PBS to reinforce the toughness of PLA; (2) the content of GVF ranged from 10 to 50 wt%, with the expected content being over 25 wt%; (3) PBS-MA and PLA-MA were added to improve the adhesion between the polymer and GVF; and (4) a lubrication agent was added to reduce viscosity and improve the dispersion of GVF in the polymer matrix.

Table 1. Formulation of samples (wt%).

Sample	PLA	PBS	GVF	PBS-MA	PLA-MA	Lubrication Agent
Pure PLA	100	--	--	--	--	--
GP-10-PBS-5	85	5	10	--	--	--
GP-20-PBS-5	75	5	20	--	--	--
GP-30-PBS-5	65	5	30	--	--	--
GP-40-PBS-5	55	5	40	--	--	--
GP-40-PBS-3	57	3	40	--	--	--
GP-50-PBS-5	45	5	50	--	--	--
GP-30-PBS-5-PBS-MA-1	64	5	30	1	--	--
GP-30-PBS-5-PBS-MA-3	62	5	30	3	--	--
MPG-30-5	62	5	30	--	3	--
AMPG-30-5	61.997	5	30	--	3	0.003

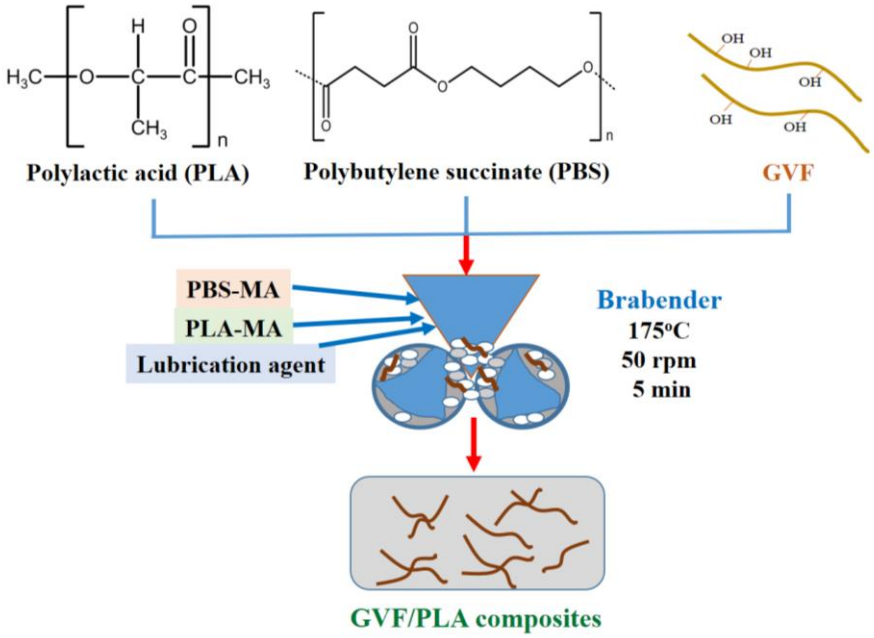

Figure 4. Preparation of GVF/PLA composites.

2.6. Thermal Analysis

A GT-HV 2000 analyzer was utilized to determine the heat deflection temperature (HDT) of pure PLA and GVF/PLA composites. The test specimen, with dimensions of 130 mm × 13 mm × 3.2 mm, was heated under a pressure of 66 psi for the thermal deformation test, at a heating rate of 2 °C/min. The test was concluded when the deformation reached 0.25 mm, in accordance with ASTM D648 [36] specifications.

2.7. Mechanical Property Test

Before mechanical testing, pure PLA and GVF/PLA composites were conditioned at 65% relative humidity and 23 °C until they reached equilibrium moisture content. For each sample, at least five specimens were tested, all at room temperature. Tensile testing was conducted using an Instron universal tester, model HT-9102 (Hung Ta Instrument Co., Taipei, Taiwan), following the ASTM D638 [36] test method at a strain rate of 50 mm/min, with a dumbbell-shaped specimen prepared according to the specified requirements. Additionally, the notched Izod impact strength was determined using a specimen measuring 64 mm × 13 mm × 3.2 mm and an impact resistance testing machine, model GT-70,045-MDL (Gotech Testing Machines Co., Taichung, Taiwan), in accordance with the ASTM D256 [36] test method.

2.8. Melt Flow Index

The melt flow index (MFI) measurements were conducted in accordance with ASTM D1238 [36], using a temperature of 210 °C and a load of 2.16 kg. Five measurements were taken for each sample, and the average values were calculated.

2.9. Morphological Analysis

The morphology of the composites was studied on the fractured surfaces after mechanical testing to observe the distribution of the GVF in the PLA matrix. This analysis was performed using a Hitachi scanning electron microscope (SEM; model S3000 N) after the sample surfaces were sputter-coated with gold to minimize the risk of charging and thermal damage.

3. Results and Discussion

3.1. GVF/PLA Composites with Different Content of PBS Subsection

As illustrated in Table 2 and Figure 5, the impact strength, tensile strength, and heat deflection temperature (HDT) of the sample containing 5% PBS and 40% GVF (GP-40-PBS-5), with values of 14.61 J/m, 24.99 MPa, and 126.35 °C, respectively, were higher than those of the sample containing 3% PBS and 40% GVF (GP-40-PBS-3), which had values of 14.19 J/m, 9.85 MPa, and 124.13 °C. Therefore, the subsequent formulation will incorporate 5% PBS into the sample.

Table 2. Mechanical and thermal properties of GVF/PLA composites.

Sample	Impact Strength (J/m)	Tensile Strength (MPa)	HDT (°C)	Melt Flow Index (g/10 min)
Pure PLA	17.47 ± 0.37	49.74 ± 0.57	57.75 ± 0.20	6.50 ± 0.005
GP-10-PBS-5	29.70 ± 0.51	54.46 ± 0.98	61.37 ± 1.01	16.17 ± 0.003
GP-20-PBS-5	18.67 ± 0.59	40.72 ± 3.04	61.40 ± 1.37	20.37 ± 0.001
GP-30-PBS-5	17.54 ± 0.25	36.24 ± 4.59	62.80 ± 0.30	22.44 ± 0.004
GP-40-PBS-5	14.61 ± 0.16	24.99 ± 2.43	126.35 ± 2.52	8.33 ± 0.005
GP-40-PBS-3	14.19 ± 0.92	9.85 ± 1.83	124.13 ± 0.74	11.76 ± 0.005
GP-50-PBS-5	14.13 ± 0.37	7.16 ± 1.41	121.64 ± 4.68	7.62 ± 0.005
GP-30-PBS-5-PBS-MA-1	17.07 ± 1.89	30.66 ± 3.39	57.78 ± 2.87	22.85 ± 0.004
GP-30-PBS-5-PBS-MA-3	15.40 ± 1.63	25.03 ± 3.73	57.49 ± 1.61	23.09 ± 0.002
MPG-30-5	24.48 ± 5.49	36.00 ± 3.92	64.60 ± 0.40	8.94 ± 0.004
AMPG-30-5	25.52 ± 1.09	45.30 ± 3.57	60.13 ± 1.52	19.73 ± 0.001

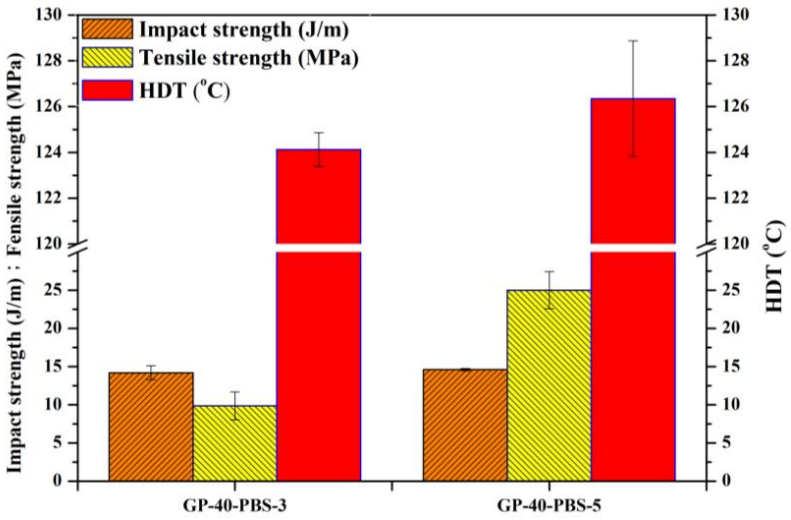

Figure 5. Mechanical and thermal properties of GVF/PLA composites with different content of PBS.

3.2. GVF/PLA Composites with Different Content of GVF

The impact strength results presented in Table 2 and Figure 6 indicate that the impact strengths of GP-10-PBS-5 (29.70 J/m), GP-20-PBS-5 (18.67 J/m), and GP-30-PBS-5 (17.54 J/m) surpassed that of pure PLA (17.47 J/m), with GP-10-PBS-5 demonstrating the highest strength. The diminished impact strength of PLA can be attributed to its inherent brittleness; thus, incorporating a softer polymer such as PBS can enhance the toughness of the composite material. Conversely, the impact strengths of GP-40-PBS-5 (14.61 J/m) and GP-50-PBS-5 (14.13 J/m) were lower than that of pure PLA (17.47 J/m). This disparity can be attributed to the uneven phase dispersion resulting from the excess GVF addition. Additionally, the impact strength decreased with increasing GVF content, likely due to the high rigidity of the fiber in GVF, which reinforces the stiffness of the composites rather than their toughness.

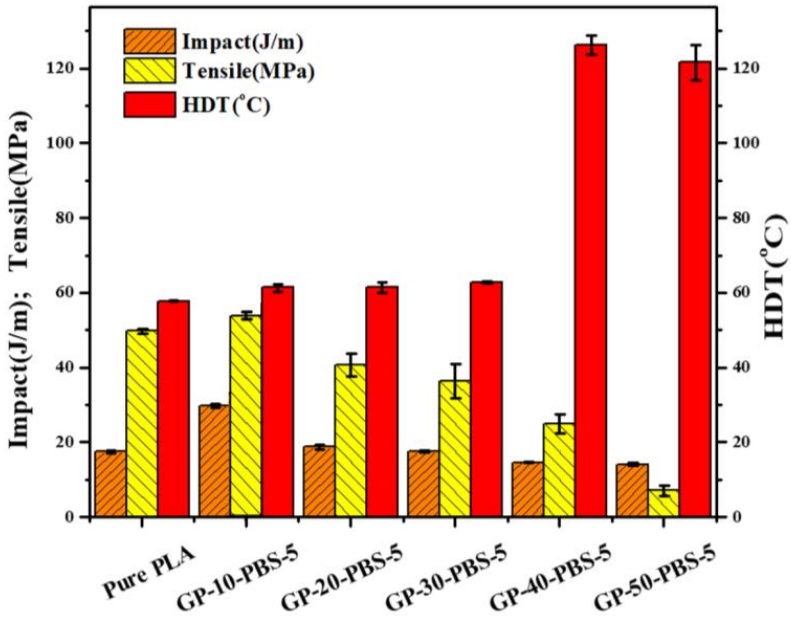

Figure 6. Mechanical and thermal properties of GVF/PLA composites with different content of GVF.

Table 2 and Figure 6 also reveal that only the tensile strength of GP-10-PBS-5 (54.46 MPa) exceeds that of pure PLA (49.74 MPa). This can be attributed to the addition of PBS, a softer polymer, which generally contributes less to tensile strength. It was observed that the tensile strength tends to decrease as the content of GVF increases. This decrease is attributed to the unmodified nature of GVF, leading to poor interfacial compatibility with the polymers and resulting in uneven dispersion, especially with excessive additions [37].

The heat deflection temperature (HDT) of pure PLA is 57.75 °C, while that of the composites is increased to over 60 °C. Moreover, the HDTs of GP-40-PBS-5 and GP-50-PBS-5 reach 126.35 °C and 121.64 °C, respectively. This increase is attributed to the fact that when the fiber content exceeds 40 wt%, the volume of GVF (which has a lower density) becomes larger than that of PLA, resulting in a phase change that allows GVF to become the continuous phase. Additionally, the rigid nature of GVF effectively reinforces the stiffness of the composites, thereby reducing material deformation and increasing the HDT.

From the points discussed, it can be concluded that, without the addition of any compatibilizers, the composite containing 10% GVF and 5% PBS exhibited the best mechanical properties. These properties gradually declined with the increase in GVF content, attributable to the uneven dispersion of GVF within the polymer matrix. Because the content of GVF reached 40 wt%, the mechanical properties decreased dramatically. Therefore, to enhance the biomass content and achieve balanced properties, we have selected composites with 30% GVF and 5% PBS (GP-30-PBS-5) for further modification.

3.3. GVF/PLA Composites Modified with PBS-MA

Table 2 and Figure 7 illustrate the impact of incorporating 3% or 1% PBS-MA on the properties of GP-30-PBS-5. The addition of 3% or 1% PBS-MA led to a reduction in the tensile strengths of the samples, dropping from 36.24 MPa for GP-30-PBS-5 to 25.03 MPa and 30.66 MPa, respectively. Furthermore, there was a decrease in the HDT, from 62.80 °C to 57.78 °C and 57.49 °C, and in the impact strength, from 17.54 J/m to 15.40 J/m and 17.07 J/m, respectively. These findings indicate that PBS-MA did not enhance the interfacial adhesion between GVF and PLA.

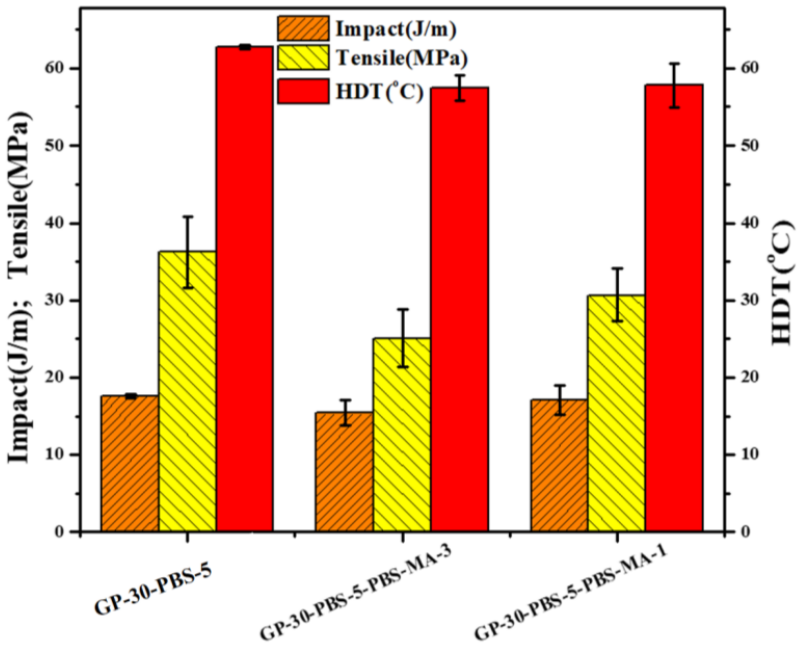

Figure 7. Mechanical and thermal properties of GVF/PLA composites modified with PBS-MA.

3.4. GVF/PLA Composites Modified with PLA-MA

Building upon GP-30-PBS-5, 3% PLA-MA (MPG-30-5) was incorporated as a compatibilizer to enhance the mechanical properties of the composite. According to Table 2 and Figure 8, the addition of PLA-MA resulted in no significant change in tensile strength (36.24 and 36.00 MPa). However, there were notable improvements in impact strength and HDT of GP-30-PBS-5, increasing from 17.54 J/m and 62.80 °C to 24.48 J/m and 64.60 °C, respectively. These findings suggest that PLA-MA improves the interfacial adhesion between the GVF and the polymer matrix more effectively than PBS-MA does. The interactions among PLA, PLA-MA, and GVF are depicted in Figure 9.

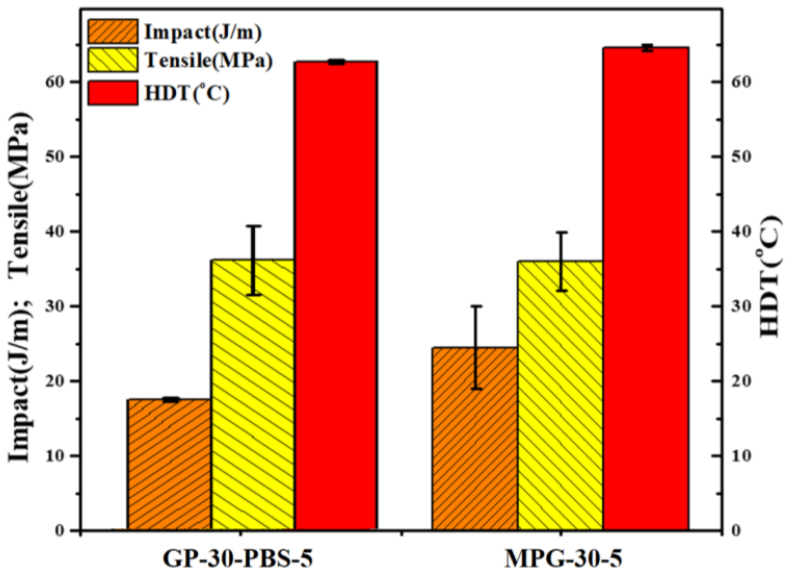

Figure 8. Mechanical and thermal properties of GVF/PLA composites modified with PLA-MA.

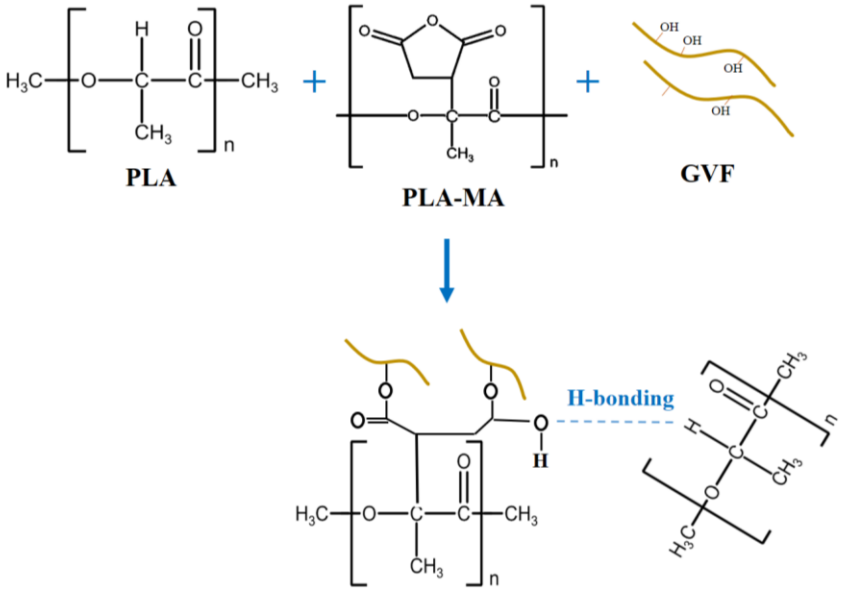

Figure 9. Interactions between PLA, PLA-MA, and GVF.

3.5. GVF/PLA Composites Modified with Lubrication Agent

Even though the addition of PLA-MA (MPG-30-5) improved the impact strength and HDT of GP-30-PBS-5, it did not enhance the tensile strength of the composite. It was discovered that while the incorporation of PLA-MA boosted compatibility between GVF and PLA, it also increased the viscosity. This higher viscosity led to an uneven dispersion of GVF, thus hindering a significant increase in tensile strength. Consequently, a lubrication agent was introduced to the MPG-30-5 composite to reduce the friction between the matrix and additives, and to lower the material's viscosity. Table 2 and Figure 10 showed that the impact and tensile strengths of the lubrication agent-containing composite (AMPG-30-5) increased from 24.48 J/m and 36.00 MPa to 25.52 J/m and 45.30 MPa, respectively. The results indicate that the impact of the lubrication agent on the increase in tensile strength is more pronounced than its effect on impact strength. This observation suggests that the uniform dispersion of the filler within the matrix is crucial in determining the tensile strength [15]. However, the HDT decreased due to the lubricating effect of the lubrication agent.

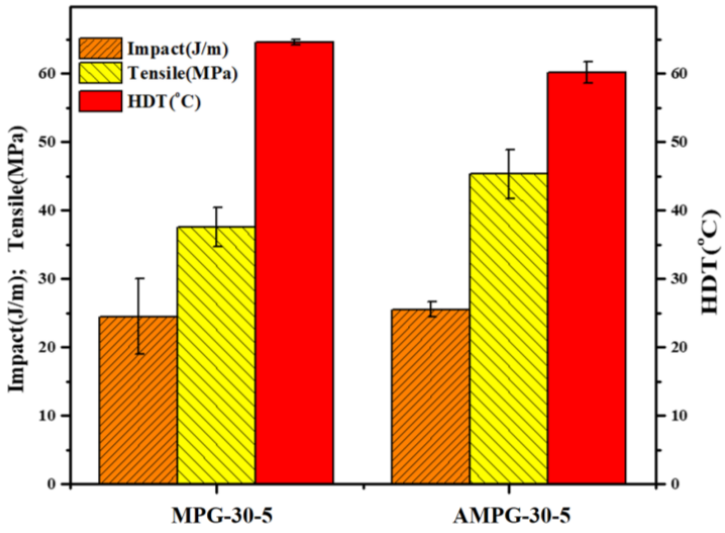

Figure 10. Mechanical and thermal properties of GVF/PLA composites modified with PLA-MA and lubrication agent.

3.6. Melt Flow Index (MFI) of GVF/PLA Composites

One of the most important measurements conducted under industrial conditions for evaluating thermoplastic polymer processing properties is the determination of the melt flow index (MFI). The results of the MFI evaluation are presented in Table 2. An increase in the MFI was observed with the addition of GVF, especially in the composites containing 10, 20, and 30 wt% of GVF, excluding MPG-30-5, with values ranging from 16.17 to 23.09, more than double that of the virgin PLA (6.50 g/10 min). Barczewski's study [38] also reported that the MFI value increases with the addition of ground chestnut shell, with the sample containing 30 wt% of ground chestnut shell showing an MFI value over five times higher than that of the neat resin. It is believed that the hydrophilic nature of plant fibers induces the hydrolytic degradation of PLA, reducing the polymer's molecular weight, which in turn facilitates flow [39]. Additionally, a scanning electron micrograph (Figure 11) of PBS-MA modified composites (GP-30-PBS-5-PBS-MA-1 and GP-30-PBS-5-PBS-MA-3) showed poor interaction between GVF and PLA, which could explain the higher flow capability observed (22.85 and 23.09 g/10 min). On the other hand, the addition of PLA-MA caused a decrease in the MFI value to 8.94, indicating that stronger bonding hinders the flow. When larger amounts of GVF were added (40 and 50 wt%), the MFI decreased to 7.62 g/10 min and 11.76 g/10 min. This is likely because the volume of GVF exceeded that of PLA, leading to a phase transition where GVF became the continuous phase, restricting the mobility of PLA and thereby reducing the flow rate.

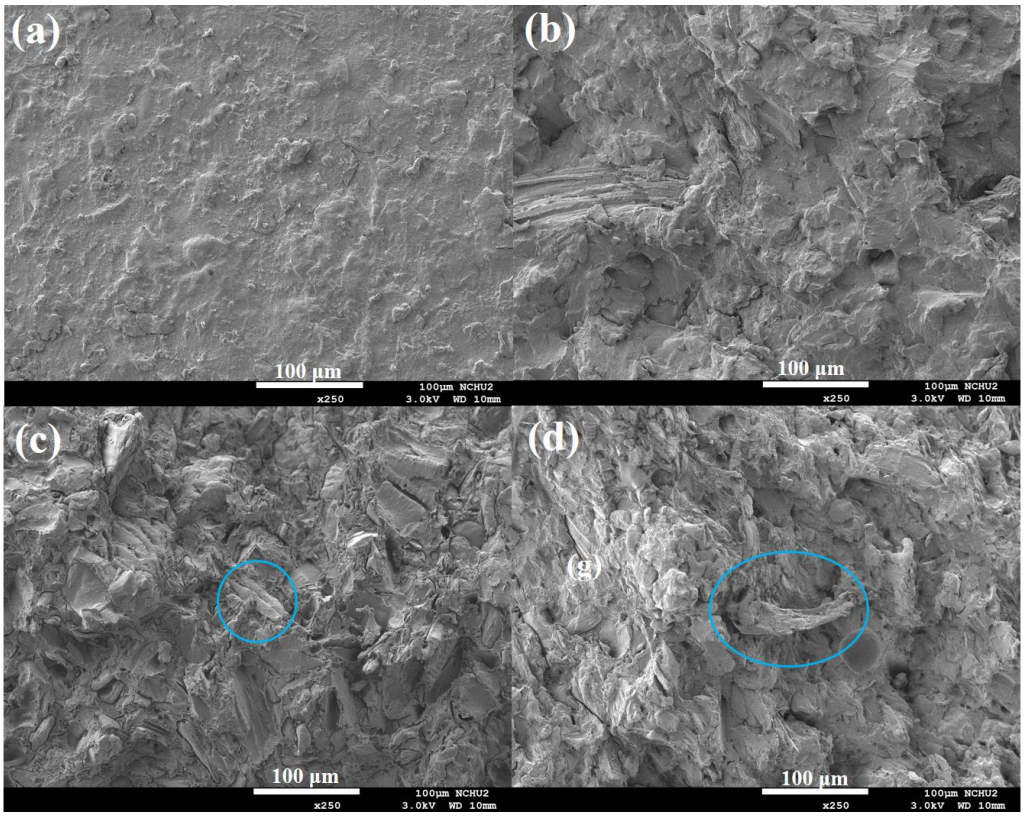

Figure 11. *Cont.*

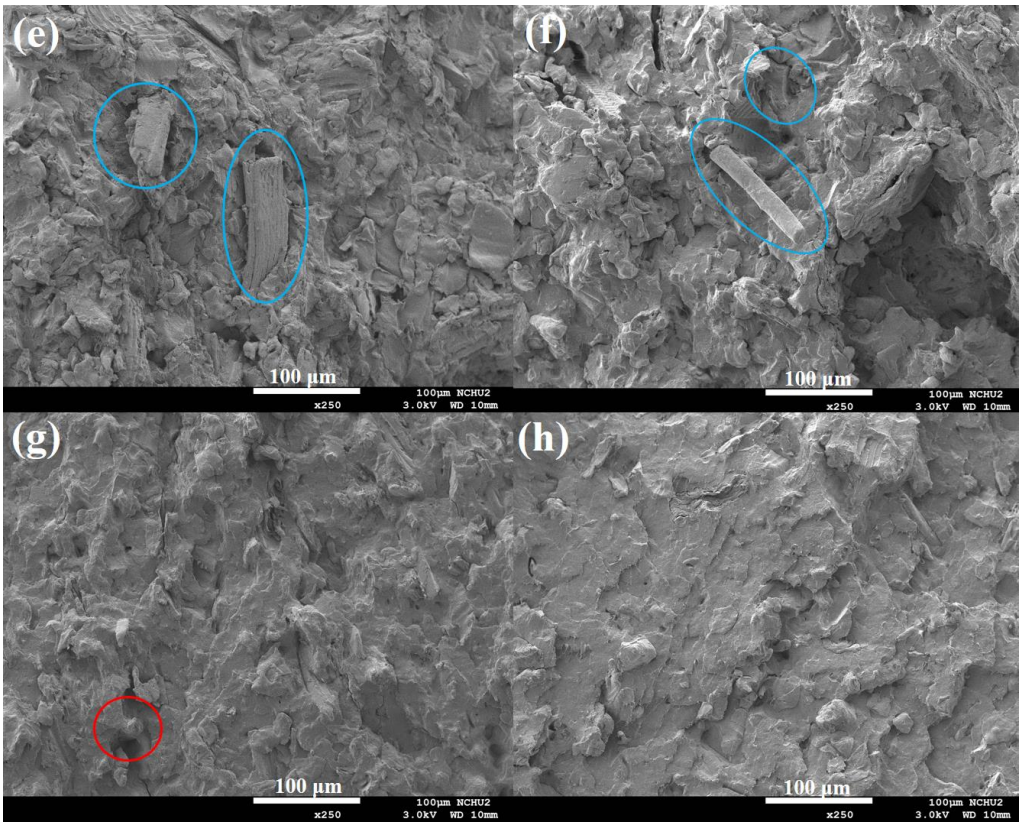

Figure 11. SEM images of PLA and its composites: (**a**) PLA, (**b**) GP-10-PBS-5, (**c**) GP-30-PBS-5, (**d**) GP-40-PBS-5, (**e**) GP-40-PBS-3, (**f**) GP-30-PBS-5-PBS-MA-3, (**g**) MPG-30-5, (**h**) AMPG-30-5.

3.7. Morphology Analysis of GVF/PLA Composites

The SEM images of the fracture surfaces of PLA and its composites are presented in Figure 11. These observations were made to confirm the earlier explanation of the rheological data based on the phenomena of compatibility and viscosity in the GVF/PLA composites. A smooth surface was observed for pristine PLA (Figure 11a). The image of GP-10-PBS-5 (Figure 11b), representing the composite with 10% GVF, shows that the GVF fibers were well-dispersed within the polymer matrix without forming agglomerated structures. In contrast, Figure 11c shows agglomerated and exposed fibers (highlighted by the blue circle) that were not fully covered by the PLA matrix in the GP-30-PBS-5 composite. Figure 11d,e display the surfaces of composites containing 40% GVF with 5% and 3% PBS (GP-40-PBS-5 and GP-40-PBS-3, respectively). Both images reveal exposed fibers (highlighted by blue circles), but GP-40-PBS-3 had more exposed fibers than GP-40-PBS-5, suggesting that 5% PBS provides better coverage. This observation aligns with the mechanical property analysis. In Figure 11f, it is evident that the addition of PBS-MA in GP-30-PBS-5-PBS-MA-3 did not improve the compatibility between GVF and PLA, as exposed fibers (marked by blue circles) are still visible. Conversely, Figure 11g shows a densely knitted texture (highlighted by the red circle), indicating that the addition of PLA-MA in MPG-30-5 improved the compatibility between the GVF and the PLA matrix, enhancing adhesion. Furthermore, the smoother texture and absence of exposed fibers in AMPG-30-5 (Figure 11h) suggest that the addition of a lubricating agent reduced the viscosity of the composite, leading to a more uniform dispersion and coverage of GVF within the PLA matrix. These microscopic observations are consistent with the results from the mechanical property and MFI analyses.

4. Conclusions

The results demonstrated that the impact of adding 5% PBS on the thermal and mechanical properties of the GVF/PLA composites was more pronounced than that of adding 3% PBS. Additionally, the tensile strength of the composite containing 10% GVF and 5% PBS (GP-10-PBS-5) reached 54.46 MPa, marking an increase of 9.5%. However, as the GVF content increased, there was a tendency for the strength to decrease. This is attributed to the poor interfacial compatibility of GVF with polymers, where excessive addition can lead to uneven dispersion. Nonetheless, the HDT of the composites increases with the GVF content, reaching 121~126 °C when the GVF content exceeds 40 wt%. This increase is due to the dominant presence of GVF in the composites, causing a phase change. Moreover, the rigid nature of the continuous phase (GVF) effectively minimizes material deformation, thereby increasing the HDT. It has also been demonstrated that using PLA-MA as a compatibilizer yields better performance than using PBS-MA. Conversely, adding PLA-MA improved the compatibility between the GVF and PLA, albeit at the cost of increased viscosity. In comparison with another study [26] that used PLA-MA in hybrid fiber/PLA composites, including oil palm empty fruit bunch fiber (EFBF) and Kenaf core fiber (KCF), it was found that the tensile strength of the composite decreased from 35.59 MPa to 30.92 MPa, while the impact strength increased from 12.29 J/m to 16.12 J/m with the addition of PLA-MA. This finding aligns with our results, which indicate that while the incorporation of PLA-MA enhanced compatibility between GVF and PLA, it also increased viscosity. This higher viscosity resulted in uneven dispersion of GVF, thereby hindering the reinforcing effect on tensile strength. In this study, the mechanical strengths of the GVF/PLA composites were further enhanced by incorporating a lubricant, which promoted better dispersion of GVF within the PLA matrix by reducing intermolecular friction forces and viscosity. The benefits of these composites extend beyond merely reducing the quantity of polymer required; they also enhance the mechanical and thermal properties of PLA. Moreover, they fulfill the objective of environmental sustainability by repurposing waste grapevines into high-value, eco-friendly bio-composites. When the GVF content exceeds 30%, and with modification by PBS, PLA-MA, and lubricants, excellent GVF bio-composites can be obtained, which can be used in the future for facilities needed for growing grapes or other plants.

Author Contributions: Conceptualization, Y.-F.S.; methodology and validation, C.-W.C. and C.-C.H.; data curation, Y.-J.J. and P.-H.W.; writing—original draft preparation, Y.-J.J. and P.-H.W.; writing—review and editing, Y.-F.S. and C.-W.C.; supervision, Y.-F.S. All authors have read and agreed to the published version of the manuscript.

Funding: This research was funded by Ministry of Science and Technology of Taiwan, grant number MOST110-2622-E-324-003.

Data Availability Statement: Data are contained within the article.

Conflicts of Interest: The authors declare no conflicts of interest.

References

1. Abdollahi Saadatlu, E.; Barzinpour, F.; Yaghoubi, S. A Sustainable Model for Municipal Solid Waste System Considering Global Warming Potential Impact: A Case Study. *Comput. Ind. Eng.* **2022**, *169*, 108127. [CrossRef]
2. Agapkin, A.M.; Makhotina, I.A.; Ibragimova1, N.A.; Goryunova, O.B.; Izembayeva, A.K.; Kalachev, S.L. The Problem of Agricultural Waste and Ways to Solve It. *IOP Conf. Ser. Earth Environ. Sci.* **2022**, *981*, 022009. [CrossRef]
3. Zulkifli, A.A.; Mohd Yusoff, M.Z.; Abd Manaf, L.; Zakaria, M.R.; Roslan, A.M.; Ariffin, H.; Shirai, Y.; Hassan, M.A. Assessment of Municipal Solid Waste Generation in Universiti Putra Malaysia and Its Potential for Green Energy Production. *Sustainability* **2019**, *11*, 3909. [CrossRef]
4. Peng, X.; Jiang, Y.; Chen, Z.; Osman, A.I.; Farghali, M.; Rooney, D.W.; Yap, P.-S. Recycling Municipal, Agricultural and Industrial Waste into Energy, Fertilizers, Food and Construction Materials, and Economic Feasibility: A Review. *Environ. Chem. Lett.* **2023**, *21*, 765–801. [CrossRef]
5. Duque-Acevedo, M.; Belmonte-Ureña, L.J.; Cortés-García, F.J.; Camacho-Ferre, F. Agricultural Waste: Review of the Evolution, Approaches and Perspectives on Alternative Uses. *Glob. Ecol. Conserv.* **2020**, *22*, E00902. [CrossRef]

6. Ramesh, P.; Singh, A.C. Chapter 1—Sources of Atmospheric Pollution in India. In *Asian Atmospheric Pollution*; Elsevier: Amsterdam, The Netherlands, 2022; pp. 1–37.
7. Glasser, W.G. About Making Lignin Great Again-Some Lessons from the Past. *Front. Chem.* **2019**, *7*, 565. [CrossRef]
8. Ruggieri, L.; Cadena, E.; Martínez-Blanco, J.; Gasol, C.M.; Rieradevall, J.; Gabarrell, X.; Gea, T.; Sort, X.; Sánchez, A. Recovery of Organic Wastes in the Spanish Wine Industry. Technical, Economic and Environmental Analyses of the Composting Process. *J. Clean. Prod.* **2009**, *17*, 830–838. [CrossRef]
9. Martínez Salgado, M.M.; Ortega Blu, R.; Janssens, M.; Fincheira, P. Grape Pomace Compost as a Source of Organic Matter: Evolution of Quality Parameters to Evaluate Maturity and Stability. *J. Clean. Prod.* **2019**, *216*, 56–63. [CrossRef]
10. Turning Winery Waste into Compost, Composting of Grape Stalks, Lees and Sludges. Available online: https://compost-turner.net/composting-technologies/grape-stalks-and-pomace-composting-process.html (accessed on 15 December 2023).
11. Available online: https://news.ltn.com.tw/news/life/breakingnews/3797880 (accessed on 11 January 2022).
12. Ngaowthong, C.; Boruvka, M.; Behalek, L.; Lenfeld, P.; Svec, M.; Dangtungee, R.; Siengchin, S.; Rangappa, S.M.; Parameswaranpillai, J. Recycling of Sisal Fiber Reinforced Polypropylene and Polylactic Acid Composites: Thermo-Mechanical Properties, Morphology, and Water Absorption Behavior. *Waste Manag.* **2019**, *97*, 71–81. [CrossRef]
13. Battegazzore, D.; Noori, A.; Frache, A. Natural Wastes as Particle Filler for Poly(Lactic Acid)-Based Composites. *J. Compos. Mater.* **2018**, *53*, 783–797. [CrossRef]
14. Komal, U.K.; Lila, M.K.; Singh, I. Pla/Banana Fiber Based Sustainable Biocomposites: A Manufacturing Perspective. *Compos. Part B Eng.* **2020**, *180*, 107535. [CrossRef]
15. Huang, C.-C.; Chang, C.-W.; Chen, C.; Shih, Y.-F. Developing Carbon-Storing Materials through Grapevine Char/Polybutylene Succinate Green Bio-Composites. *Compos. Part C Open Access* **2024**, *13*, 100442. [CrossRef]
16. Oliver-Ortega, H.; Reixach, R.; Espinach, F.X.; Mendez, J.A. Maleic Anhydride Polylactic Acid Coupling Agent Prepared from Solvent Reaction: Synthesis, Characterization and Composite Performance. *Materials* **2022**, *15*, 1161. [CrossRef]
17. Almeida, V.H.M.; Jesus, R.M.; Santana, G.M.; Pereira, T.B. Polylactic Acid Polymer Matrix (Pla) Biocomposites with Plant Fibers for Manufacturing 3d Printing Filaments: A Review. *J. Compos. Sci.* **2024**, *8*, 67. [CrossRef]
18. Hassan, E.; Wei, Y.; Jiao, H.; Huo, Y. Plant Fibers Reinforced Poly (Lactic Acid) (Pla) as a Green Composites: Review. *Int. J. Eng. Sci. Technol.* **2012**, *4*, 4429–4439.
19. Bumbudsanpharoke, N.; Wongphan, P.; Promhuad, K.; Leelaphiwat, P.; Harnkarnsujarit, N. Morphology and Permeability of Bio-Based Poly(Butylene Adipate-Co-Terephthalate) (Pbat), Poly(Butylene Succinate) (Pbs) and Linear Low-Density Polyethylene (Lldpe) Blend Films Control Shelf-Life of Packaged Bread. *Food Control* **2022**, *132*, 108541. [CrossRef]
20. Aliotta, L.; Seggiani, M.; Lazzeri, A.; Gigante, V.; Cinelli, P. A Brief Review of Poly (Butylene Succinate) (Pbs) and Its Main Copolymers: Synthesis, Blends, Composites, Biodegradability, and Applications. *Polymers* **2022**, *14*, 844. [CrossRef]
21. Su, S.; Kopitzky, R.; Tolga, S.; Kabasci, S. Polylactide (Pla) and Its Blends with Poly(Butylene Succinate) (Pbs): A Brief Review. *Polymers* **2019**, *11*, 1193. [CrossRef]
22. Zhang, M.; Jiang, C.; Wu, Q.; Zhang, G.; Liang, F.; Yang, Z. Poly(Lactic Acid)/Poly(Butylene Succinate) (Pla/Pbs) Layered Composite Gas Barrier Membranes by Anisotropic Janus Nanosheets Compartibilizers. *ACS Macro Lett.* **2022**, *11*, 657–662. [CrossRef]
23. Shih, Y.F.; Xu, J.Y.; Wu, N.Y.; Chiu, Y.T.; Yu, H.M.; Tsai, M.L. Eco-Friendly Composites Based on Bitter Tea Oil Meal and Polylactic Acid. *Key Eng. Mater.* **2021**, *889*, 21–26. [CrossRef]
24. Karimah, A.; Ridho, M.R.; Munawar, S.S.; Adi, D.S.; Ismadi; Damayanti, R.; Subiyanto, B.; Fatriasari, W.; Fudholi, A. A Review on Natural Fibers for Development of Eco-Friendly Bio-Composite: Characteristics, and Utilizations. *J. Mater. Res. Technol.* **2021**, *13*, 2442–2458. [CrossRef]
25. Yang, Z.; Feng, X.; Xu, M.; Rodrigue, D. Properties of Poplar Fiber/Pla Composites: Comparison on the Effect of Maleic Anhydride and Kh550 Modification of Poplar Fiber. *Polymers* **2020**, *12*, 729. [CrossRef] [PubMed]
26. Birnin-Yauri, A.U.; Ibrahim, N.A.; Zainuddin, N.; Abdan, K.; Then, Y.Y.; Chieng, B.W. Effect of Maleic Anhydride-Modified Poly(Lactic Acid) on the Properties of Its Hybrid Fiber Biocomposites. *Polymers* **2017**, *9*, 165. [CrossRef]
27. González-López, M.E.; Robledo-Ortíz, J.R.; Manríquez-González, R.; Silva-Guzmán, J.A.; Pérez-Fonseca, A.A. Polylactic Acid Functionalization with Maleic Anhydride and Its Use as Coupling Agent in Natural Fiber Biocomposites: A Review. *Compos. Interfaces* **2018**, *25*, 515–538. [CrossRef]
28. Rojas-Lema, S.; Arevalo, J.; Gomez-Caturla, J.; Garcia-Garcia, D.; Torres-Giner, S. Peroxide-Induced Synthesis of Maleic Anhydride-Grafted Poly(Butylene Succinate) and Its Compatibilizing Effect on Poly(Butylene Succinate)/Pistachio Shell Flour Composites. *Molecules* **2021**, *26*, 5927. [CrossRef]
29. Hamdiani, S.; Shih, Y.F. Development of Polylactic Acid-Polybutylene Succinate-Silver Nanoparticle-Diatomite (Plapbs-Agnps-D) Composite in Different Compatibilizer as Potential Pollutants Storage Container for Methylene Blue Self-Degradation. *J. Polym. Res.* **2022**, *29*, 232. [CrossRef]
30. AL-Oqla, F.M.; Alaaeddin, M.H. Chemical Modifications of Natural Fiber Surface and Their Effects. In *Bast Fibers and Their Composites*; Rajeshkumar, G., Devnani, G., Sinha, S., Sanjay, M., Siengchin, S., Eds.; Springer: Singapore, 2022.
31. Thamarai Selvi, S.; Sunitha, R.; Ammayappan, L.; Prakash, C. Impact of Chemical Treatment on Surface Modification of Agave Americana Fibres for Composite Application—A Futuristic Approach. *J. Nat. Fibers* **2023**, *20*, 2142726. [CrossRef]

32. Dai, L.; Wang, X.; Zhang, J.; Wang, F.; Ou, R.; Song, Y. Effects of Lubricants on the Rheological and Mechanical Properties of Wood Flour/Polypropylene Composites. *J. Appl. Polym. Sci.* **2019**, *136*, 47667. [CrossRef]
33. Hosseini, S.; Venkatesh, A.; Boldizar, A.; Westman, G. Molybdenum Disulphide—A Traditional External Lubricant That Shows Interesting Interphase Properties in Pulp-Based Composites. *Polym. Compos.* **2021**, *42*, 4884–4896. [CrossRef]
34. Beta Analytic. Available online: https://www.betalabservices.com/biobased/biomasspla.html (accessed on 25 August 2024).
35. Hwang, S.W.; Lee, S.B.; Lee, C.K.; Lee, J.Y.; Shim, J.K.; Selke, S.E.M.; Soto-Valdez, H.; Matuana, L.; Rubino, M.; Auras, R. Grafting of Maleic Anhydride on Poly(L-Lactic Acid). Effects on Physical and Mechanical Properties. *Polym. Test.* **2012**, *31*, 333–344. [CrossRef]
36. Available online: https://www.astm.org/products-services/standards-and-publications/standards/plastics-standards.html (accessed on 10 December 2022).
37. Babu, S.; Singh Rathore, S.; Singh, R.; Kumar, S.; Singh, V.K.; Yadav, S.K.; Yadav, V.; Raj, R.; Yadav, D.; Shekhawat, K.; et al. Exploring Agricultural Waste Biomass for Energy, Food and Feed Production and Pollution Mitigation: A Review. *Bioresour. Technol.* **2022**, *360*, 127566. [CrossRef] [PubMed]
38. Barezewski, M.; Mysiukiewicz, O. Rheological and Processing Properties of Poly(Lactic Acid) Composites Filled with Ground Chestnut Shell. *Polym. Korea* **2018**, *42*, 267–274. [CrossRef]
39. Lee, C.H.; Sapuan, S.M.; Lee, J.H.; Hassan, M.R. Melt Volume Flow Rate and Melt Flow Rate of Kenaf Fibre Reinforced Floreon/Magnesium Hydroxide Biocomposites. *Springerplus* **2016**, *5*, 1680. [CrossRef] [PubMed]